

Raman Modes of 6H Polytype of Silicon Carbide to Ultrahigh Pressures: A Comparison with Silicon and Diamond

Jun Liu and Yogesh K. Vohra

Department of Physics, University of Alabama at Birmingham, Birmingham, Alabama 35294-1170
(Received 10 January 1994; revised manuscript received 17 March 1994)

We report the Raman study on 6H-SiC to ultrahigh pressures of 95 GPa in a diamond anvil cell. The LO(Γ) and TO(Γ) Raman frequencies increase with increasing pressures. A very interesting turnaround in the LO-TO splitting is observed above 60 GPa. The density variation of the mode Grüneisen parameters for 6H-SiC is compared to that of silicon, cubic boron nitride, and diamond. The SiC is transparent to the visible light at 95 GPa and the anticipated metallic phase was not observed.

PACS numbers: 62.50.+p, 63.20.-e, 78.30.Hv, 81.40.Vw

The wide band gap semiconductor silicon carbide (SiC) is both of scientific and technological interest [1,2]. The technological interests include superabrasives, high temperature electronic material, as well as blue light emitting diode (LED) [2]. The scientific interest in silicon carbide is driven by the wide variety of its polytypes (200 polytypes have been reported [3]) and their structural and electronic properties. SiC polytype can be divided into low temperature types (2H and 3C) and high temperature types (4H, 6H, etc.). 6H-SiC is of particular interest because of the large band gap (3.0 eV) and is widely regarded as an ideal material for blue LED because of the ease of impurity doping in this material. High pressure studies have been carried out in the past largely on 3C-SiC and Raman modes have been documented to 80 GPa [1, 4–6]. Theoretical study predicted a phase transition in 3C-SiC from zinc-blende structure to the rock salt phase at 66 GPa [7]. 6H-SiC polytype Raman studies were carried out only to 50 GPa [6, 8]. The present high pressure studies are motivated by the effect of reduced interatomic distances on the optical phonons in 6H-SiC to ultrahigh pressures and comparison with other superhard materials like boron nitride and diamond. Also, SiC is usually regarded as intermediate between silicon and diamond in its mechanical and electronic properties. Therefore, we compare the SiC behavior at high compression with that of silicon and diamond. Thermodynamic quantity (the mode Grüneisen parameter γ) and microscopic quantity (transverse effective charge e_T^*) in an extended pressure range have been measured for the first time. Recent x-ray diffraction studies [9] have reported a phase transition in 3C-SiC from the ZnS structure to the rock salt structure at 100 GPa with an abrupt volume reduction of 20.3%. On the other hand, 6H-SiC was found to be stable to 95 GPa with some additional diffraction lines attributed as a premonition of a phase transition. These studies are not conclusive, however, and we examine the Raman modes to investigate this possibility further.

The single crystal 6H-SiC samples of 500–100 μm in diameter were cut from the electronic grade material grown by the chemical vapor deposition (CVD) method. Three experiments were carried out at high pressures in a diamond anvil cell device. The first experiment employed large flat diamonds of 600 μm diameter with methanol:ethanol (4:1) pressure medium to 12 GPa. In the second experiment, without any medium, two diamond anvils with 200 and 300 μm diameters were employed to generate ultrahigh pressures to 95 GPa. Pressures in these two experiments were measured by the ruby pressure marker [10]. The third experiment duplicated the second experiment to 90 GPa with only a SiC plus methanol:ethanol (4:1) medium to study the pure sample, using the TO(Γ) mode calibration of experiment 2 to measure the pressure. The backscattering configuration micro-Raman system described elsewhere [11] was employed in the present experiments. The 514.5 nm argon laser beam was coupled into the diamond anvil cell and focused on the sample to a spot size of 5 μm . This is of advantage for avoiding the pressure inhomogeneity if great care was taken by obtaining the SiC Raman spectra at the same region where the ruby was also probed. Under high pressures, the sample thickness was reduced to less than 10 μm , and the laser probing volume was also reduced to $\sim 50 \mu\text{m}^3$, thus the Raman signal became much too weak to be detected. However, the fact that the sensitive liquid N₂ cooled charge coupled device detector has virtually zero thermal noise enables long exposure to detect weak signals (typical data collection time at high pressures was 1000 s at a laser power of 900 mW).

Figure 1 shows the 6H-SiC Raman spectra of the LO(Γ) and TO(Γ) modes at different pressures. The ambient pressure spectrum shows five Raman active modes in the frequency range of 700 to 1300 cm^{-1} , namely [8], a LO(Γ) mode at 969 cm^{-1} and a strong TO(Γ) mode at 789 cm^{-1} . Additional weak TO modes at 767, 798, and 888 cm^{-1} were also observed. We focus our attention on the pressure dependence of the intense TO(Γ) mode at 789 cm^{-1} and LO(Γ) mode at 969 cm^{-1} .

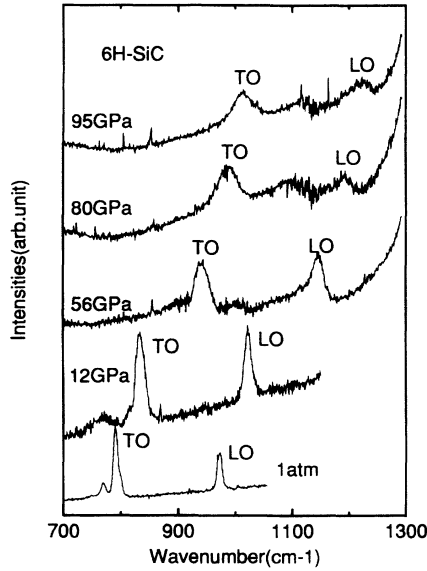


FIG. 1. Micro-Raman spectra from the 6H-SiC sample in the diamond anvil cell at various pressures. The pressures are measured by the ruby fluorescence. The strong background near 1300 cm^{-1} is due to the tail of the Raman mode of diamond anvil.

LO and TO Raman mode frequencies increase with increasing pressures (Fig. 1). At 95 GPa, the LO mode has a 253 cm^{-1} shift from its ambient pressure value of 969 to 1222 cm^{-1} , entering the tail of the strong diamond first order Raman line indicated by the high frequency background in Fig. 1. The following quadratic fits to the mode frequencies gave a satisfactory representation of our data:

$$\begin{aligned}\omega_{\text{LO}}(\text{cm}^{-1}) &= 970.1 + 3.83P - 0.013P^2, \\ \omega_{\text{TO}}(\text{cm}^{-1}) &= 789.2 + 3.11P - 0.009P^2,\end{aligned}\quad (1)$$

where P is the measured pressure in GPa.

At ultrahigh pressures over 80 GPa, there is a weak peak between the LO and TO modes, which is at 1100 cm^{-1} at 80 GPa and 1120 cm^{-1} at 95 GPa. We tentatively assign it to the axial optic mode which is a very weak mode at 888 cm^{-1} at ambient pressure, and picks up its intensity at high pressures.

Figure 2 shows the LO-TO splitting as a function of pressure. The solid line is the quadratic fit to the data from experiments 1 and 2 which had explicit pressure measurement with ruby. The upper scale is the atomic density normalized to the ambient pressure value (ρ/ρ_0) as obtained from Birch-Murnaghan's equation of state [12]. The experimental values of the bulk modulus $B_0 = 260\text{ GPa}$ and its pressure derivative $B'_0 =$ for 6H-SiC are given in Ref. [9]. The LO-TO splitting is 181 cm^{-1} at ambient pressure and increases rapidly below 60 GPa. Above 60 GPa, the splitting tends to saturate at 205 cm^{-1} . The data to 90 GPa obtained under quasi-hydro-

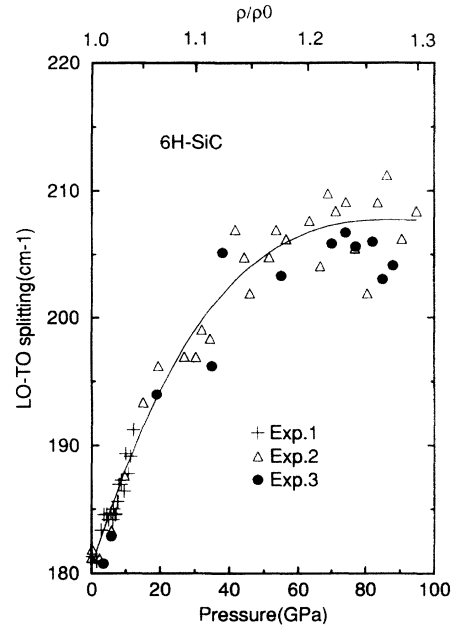


FIG. 2. The LO-TO splitting in 6H-SiC as a function of pressure. Three different experiments are described in the text. The upper scale is the density variation from the equation of state of 6H-SiC. The solid curve is the quadratic fit to the data.

drostatic (experiment 3) and to 95 GPa under presumably nonhydrostatic (experiment 2) conditions gave the same general trend of saturation in LO-TO splitting. Therefore, we believe that the saturation in LO-TO splitting and the following conclusions derived herewith are independent of the nonhydrostatic component.

The transverse effective charge e_T^* can be evaluated as [1, 13, 14]

$$\omega_{\text{LO}}^2 - \omega_{\text{TO}}^2 = \frac{2\pi e_T^{*2}}{\epsilon_\infty V M_{\text{red}}}, \quad (2)$$

where $e_T^* = e_T^*(\text{Si}) = -e_T^*(\text{C})$; M_{red} is the reduced mass of Si and C, V is the atomic volume, and ϵ_∞ is the high frequency (optical) dielectric constant. $\epsilon_\infty = 6.52$ at ambient pressure [1]. Following the method in Ref. [1], we use the relation $d \log \epsilon_\infty / d \log V \cong 0.6$ [1, 13, 15] to describe the volume dependence of ϵ_∞ , and hence the pressure dependence of ϵ_∞ , if the equation of state data [9] were applied. Combined with our LO-TO splitting data to 95 GPa (Fig. 2), we are able to experimentally determine the e_T^* value at different pressures.

Figure 3 shows the transverse effective charge e_T^* with the unit of the electron charge at different pressures. The dashed line is from Olego, Cardona, and Vogl [1]. In the low pressure range below 20 GPa, the two experimental data are in reasonable agreement considering the uncertainty in the equation of state in the earlier work [1]. It is well known that the zinc-blende-type III-V and II-VI semiconductors [16–19] show the decreases

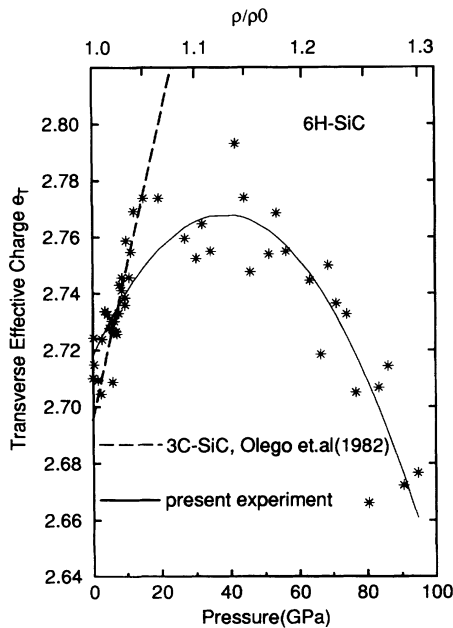


FIG. 3. The transverse effective charge (e_T^*) at various pressures. The decrease in e_T^* above 40 GPa indicates the increased covalent bonding in the material.

of e_T^* when the pressure is applied. But SiC displays a significant increase from 2.70 at ambient pressure to 2.82 at 22.5 GPa. The most significant result from Fig. 3 on the 6H-SiC measurement is that at around 40 GPa, e_T^* reaches the peak value of 2.80 but drops down beyond this pressure to 2.66 at 95 GPa. These changes in the dynamical transverse effective charge are small (1% to 2%), but nevertheless reflect changes in the electronic structure with compression. The changes in e_T^* for semiconductors have been correlated to the changes in the ionic character of the bond [1]. This may imply that 6H-SiC is more *ionic* when compressed by the pressure from 0 to 40 GPa, but is more *covalent* if even higher pressures are applied. This covalent tendency above 40 GPa is similar to other III-V and II-VI compounds at a lower pressure regime which only display a decrease of e_T^* when the pressure is applied. It was also observed that the SiC sample became transparent to the visible light at high pressures. These two phenomena are consistent, proving that the 6H-SiC phase is stable up to 95 GPa, and it has not become metallic.

However, it should be added that the charge exchange between the silicon and the carbon atom is only a small contributing factor in the LO-TO splitting. This is clearly illustrated by the fact that the total change in the LO-TO splitting is 15% between 0 and 95 GPa. On the other hand, the change in e_T^* is only 1.5%, an order of magnitude lower in the same pressure range. Hence, the pressure dependence of other parameters like ϵ_∞ and volume is the dominant factor in LO-TO splitting.

The mode Grüneisen coefficient γ can be evaluated when the LO and TO frequency data are combined with the equation of state data. γ is defined as [20]

$$\gamma_i \equiv -\frac{d \log \omega_i}{d \log V}, \quad (4)$$

where i is denoted as LO and TO, ω_i is the frequency, and V is the atomic volume. The LO and TO modes are degenerate in pure Si and C. The importance of the density variation of γ lies in the fact that the information of the mode softening with the pressure, being regarded as a precursor for the phase transition [5], can be derived from this value.

Figure 4 shows the comparison of the normalized γ for the Raman modes of silicon, cubic boron nitride (c-BN), and diamond with our result for the 6H-SiC LO and TO modes. The Grüneisen parameters of silicon and diamond as well as their density variations are from Ref. [5]. Si transforms into a β -Sn structure at 10 GPa, and diamond data are only available to 72 GPa [21]. The plots for Si and C only go to these limits. γ_0 is the ambient pressure value. For Si, $\gamma_0 = 0.98$; for c-BN [22], $\gamma_0(\text{LO}) = 0.91$, $\gamma_0(\text{TO}) = 1.20$; for diamond, $\gamma_0 = 0.97$ [5]; and our measurement for 6H-SiC, $\gamma_0(\text{LO}) = 1.23$, $\gamma_0(\text{TO}) = 1.23$. Our γ_0 for SiC agrees with earlier studies [1, 5, 7]. The method we use to obtain our result for SiC is to evaluate each $\gamma_i = \Delta \log(\omega_i) / \Delta \log(V)$ point by point with the experimental data, and fit the $\gamma_i \sim \rho/\rho_0$ curve as a linear function. The large error bars in Fig. 4 are due to the uncertainty in the second order derivative of the experimental data. However, both LO

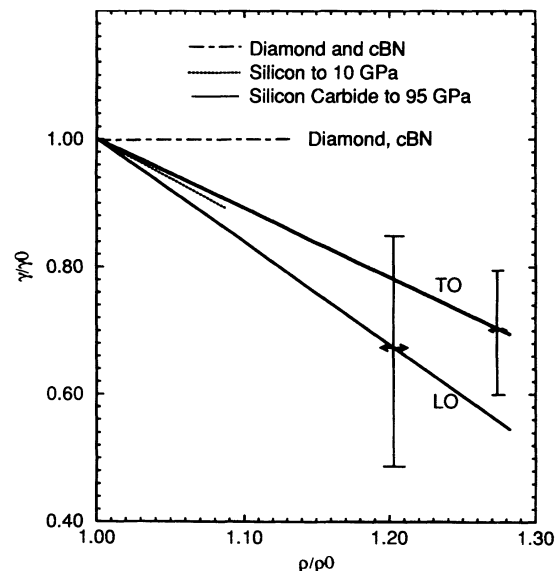


FIG. 4. The density variation of the mode Grüneisen parameters (γ) for diamond, cubic boron nitride, silicon, and 6H-silicon carbide. For diamond and silicon, LO and TO modes are degenerate. The error bars are for two data points and are representative.

and TO modes of SiC soften (γ decreases) with increasing pressure. SiC LO and TO modes behave more like the Raman mode of Si. For diamond and *c*-BN, the γ value of the corresponding Raman mode does not depend on the volume [23].

The following conclusions are obtained from the above discussions:

(1) The TO and LO modes of 6H-SiC are observed to ultrahigh pressures of 95 GPa. This indicates the structural stability of the 6H structure. The sample is optically transparent at 95 GPa. No indication of the metallic phase was observed.

(2) The transverse effective charge is found to decrease at high pressures, after increasing at lower pressures and reaching a peak value at about 40 GPa. This indicates an increasing covalent bonding at high pressures. This unique behavior agrees with the proposed theory.

(3) The mode Grüneisen parameters γ for LO and TO modes of the SiC are calculated from experimental data. By comparing the density variation of γ with diamond and Si, we conclude that the γ of the LO mode for 6H-SiC is softer than that of the TO mode, and they both show an anomalous decrease. This may be regarded as a precursor to the phase transition in the 100–200 GPa range.

This work was supported by National Science Foundation Grant No. DMR-9296212. We thank Dr. Chin Che Tin of Auburn University for providing the CVD grown 6H-SiC sample.

-
- [1] D. Olego, M. Cardona, and P. Vogl, *Phys. Rev. B* **25**, 3878 (1982).
 - [2] W. S. Yoo and H. Matsunami, *Jpn. J. Appl. Phys.* **30**, 545 (1991).
 - [3] A. Addamiano, in *Silicon Carbide—1973*, edited by R. C. Marshall, J. W. Faust, Jr., and C. E. Ryan, (University of South Carolina, Columbia, 1974), p. 179.

- [4] S. S. Mitra, O. Brafman, W. B. Daniels, and R. K. Crawford, *Phys. Rev.* **186**, 942 (1969).
- [5] A. F. Goncharov, E. V. Yakovenko, and S. M. Stishov, *JETP Lett.* **52**, 491 (1990).
- [6] I. V. Aleksandrov, A. F. Goncharov, E. V. Yakovenko, and S. M. Stishov, in *High Pressure Research: Applications to Earth and Planetary Sciences*, edited by Y. Syono and M. H. Manghnani (Terra, Tokyo, Washington, DC, 1992), p. 409.
- [7] K. J. Chang and M. L. Cohen, *Phys. Rev. B* **35**, 8196 (1987).
- [8] G. Salvador and W. F. Sherman, *J. Mol. Struct.* **247**, 373 (1991).
- [9] M. Yoshida, A. Onodera, M. Ueno, K. Takemura, and O. Shimomura, *Phys. Rev. B* **48**, 10587 (1993).
- [10] H.-k. Mao, P. M. Bell, J. W. Shaner, and D. J. Steinberg, *J. Appl. Phys.* **49**, 3276 (1978).
- [11] Y. K. Vohra and S. S. Vagarali, *Appl. Phys. Lett.* **61**, 2680 (1992).
- [12] F. Birch, *J. Geophys. Res.* **83**, 1257 (1978).
- [13] W. Harrison, *Electronic Structure and Properties of Solids* (Freeman, San Francisco, 1980).
- [14] B. A. Weinstein and R. Zallen, in *Light Scattering in Solids*, edited by M. Cardona and G. Güntherodt (Springer, Berlin, 1984), p. 463.
- [15] D. Olego and M. Cardona, *Phys. Rev. B* **25**, 1151 (1982).
- [16] J. A. Sanjurjo, E. López-Cruz, P. Vogl, and M. Cardona, *Phys. Rev. B* **28**, 4579 (1983).
- [17] B. A. Weinstein and G. J. Piermarini, *Phys. Rev. B* **46**, 1172 (1975).
- [18] R. Trommer, H. Müller, M. Cardona, and P. Vogl, *Phys. Rev. B* **21**, 4869 (1980).
- [19] B. A. Weinstein, *Solid State Commun.* **24**, 595 (1977).
- [20] N. W. Ashcroft and N. D. Mermin, *Solid State Physics* (W. B. Saunders, Philadelphia, 1976), p. 492.
- [21] I. V. Aleksandrov, A. F. Goncharov, A. N. Zisman, and S. M. Stishov, *Sov. Phys. JETP* **66**, 384 (1987).
- [22] I. E. V. Yakovenko, I. V. Aleksandrov, A. F. Goncharov, and S. M. Stishov, *Sov. Phys. JETP* **68**, 1213 (1989).
- [23] H. J. McSkimin and P. Andreatch, Jr., *J. Appl. Phys.* **43**, 2944 (1972).